Chem

CellPress

Article

DFT-Guided Phosphoric-Acid-Catalyzed Atroposelective Arene Functionalization of Nitrosonaphthalene

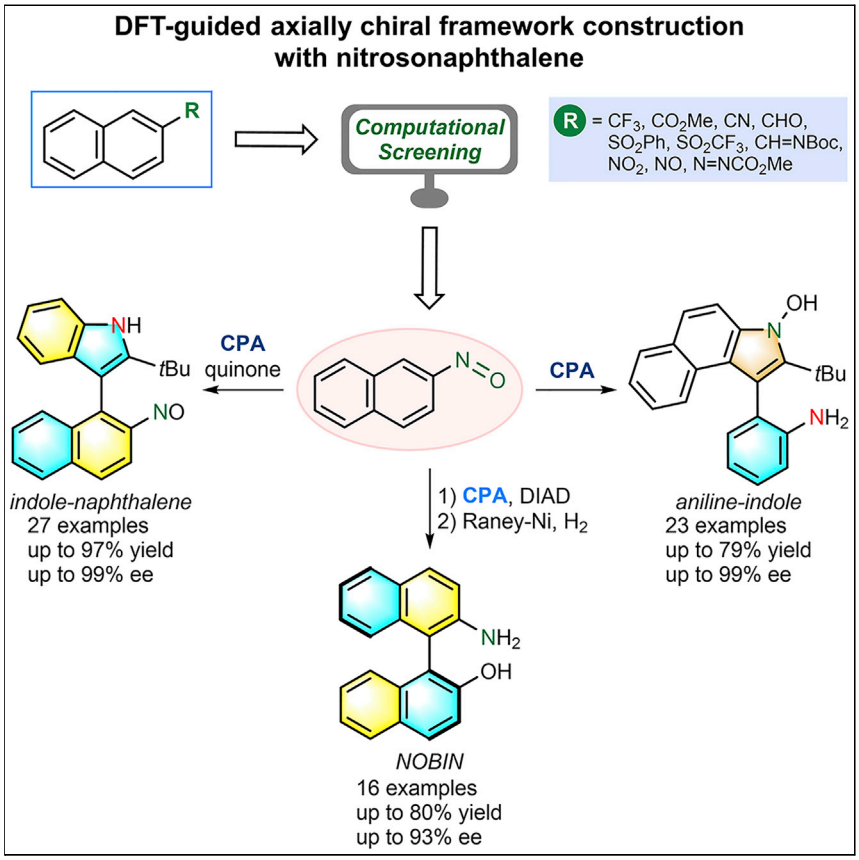

Guided by computational design, Tan and colleagues disclose a chiral phosphoric-acid-catalyzed asymmetric functionalization of naphthalenes with nitroso as the activating and directing group. This nucleophilic aromatic substitution reaction allows divergent access to two types of axially chiral arylindole frameworks with wide substrate generality under excellent enantiocontrol and, more importantly, offers a facile approach to the privileged NOBIN (2-amino-2′-hydroxy-1,1′-binaphthyl) structures. DFT calculations illustrate the plausible reaction pathway and provide additional insights into the origins of enantioselectivity.

Wei-Yi Ding, Peiyuan Yu, Qian-Jin An, ..., Ying Chen, K.N. Houk, Bin Tan

houk@chem.ucla.edu (K.N.H.)
tanb@sustech.edu.cn (B.T.)

HIGHLIGHTS

Computation-guided screening of functional groups for arene activation

Chemoselective C–H functionalization of 2-nitrosonaphthalene at an unconventional site

One-pot synthesis of optically active NOBINs by a solo organocatalytic system

Divergent access to two types of axially chiral arylindole frameworks

Ding et al., Chem 6, 2046–2059
August 6, 2020 © 2020 Elsevier Inc.
https://doi.org/10.1016/j.chempr.2020.06.001

CellPress

Chem

Article

DFT-Guided Phosphoric-Acid-Catalyzed Atroposelective Arene Functionalization of Nitrosonaphthalene

Wei-Yi Ding,[1,4] Peiyuan Yu,[1,4] Qian-Jin An,[1,4] Katherine L. Bay,[2,4] Shao-Hua Xiang,[1,3] Shaoyu Li,[1,3] Ying Chen,[1] K.N. Houk,[2,*] and Bin Tan[1,5,*]

SUMMARY

Functionalization of arenes represents the most efficient approach for constructing a core backbone of important aryl compounds. Compared with the well-developed electrophilic aromatic substitution and transition-metal-catalyzed C–H activation, nucleophilic aromatic substitution remains challenging because of the lack of a convenient route for rapid conversion of the σ^H adduct to other stable and versatile intermediates *in situ*. Guided by computational design, we were able to realize asymmetric nucleophilic aromatic substitution by introducing a nitroso group on naphthalene via chiral phosphoric acid catalysis. This strategy enables efficient construction of atropisomeric indole-naphthalenes and indole-anilines with excellent stereocontrol. Density functional theory (DFT) calculations provide further insights into the origins of enantioselectivity and the reaction mechanisms. The successful application in the synthesis of NOBINs (2-amino-2′-hydroxy-1,1′-binaphthyl) extends the utility of this strategy.

INTRODUCTION

Functionalized arene frameworks are involved in many reagents, catalysts, materials, and pharmaceuticals.[1] Electrophilic aromatic substitution reactions (via positively charged Wheland intermediates), such as the Friedel-Crafts reaction,[2–4] are the classic approach to substituted arenes (Figure 1A). Recent advances in transition-metal and photoredox catalysis have enriched the synthetic chemists' toolbox for the functionalization of different arene scaffolds.[5–11] Functionalizations via the negatively charged Meisenheimer σ^X adduct or σ^H adduct often bank on the presence of nitro substituents and nucleofugal halogen (X) or external oxidants (H), which limit applicability (Figure 1A).[12–14] Although it has been established that the formation of σ^H adducts precedes the formation of σ^X adducts,[15] we recently employed asymmetric organocatalysis[16–19] and azo groups[20] to harness the σ^H adduct and efficiently enable the functionalization of arenes with bifunctional chiral phosphoric acid[21–23] (CPA) catalysis. The azo substituent constitutes extended conjugation and electron-withdrawing capability to prime the arene for a regioselective nucleophilic attack (Figure 1B). It further serves as an oxidant to promote expeditious intramolecular conversion of the σ^H adduct intermediate to outcompete the formation of the σ^X adduct. To further extend this concept and bring about a more universal synthetic tool for arene functionalization, one could, in principle, utilize substrates possessing substituents with electronic properties similar to those of the azo group. With the help of electronic structure calculations on a series of naphthalene

The Bigger Picture

Highly efficient conversion of inexpensive and readily available arene materials into high-value-added chiral molecules is of great importance in modern synthetic chemistry given the enormous potential of such structures in functional materials, pharmaceuticals, and other relevant chemical industries. Organocatalytic nucleophilic aromatic substitution enabled by an azo group offers an effective approach to enantioselective functionalization of naphthalene C–H bonds featuring an intramolecular oxidation of an unstabilized σ^H adduct. Premised on density functional theory (DFT) calculations, nitroso has emerged as another promising activating and oxidative group, whose synthetic potential is substantiated in the atroposelective synthesis of several groups of representative biaryl atropisomers processed by a chiral phosphoric acid catalyst. The success of this reaction explicitly exemplifies the ability of computational tools to streamline organic synthesis with intensified robustness in the disclosed strategy.

derivatives, we found that a nitroso group exhibits great potential for such a transformation (Figure 1C).

RESULTS AND DISCUSSION

Preliminary Computational Screening

On the basis of these considerations, a series of substituted naphthalenes were designed and subjected to preliminary computational screening in search of optimal substrate models for catalytic asymmetric nucleophilic aromatic substitution.[24–26] We reasoned that the reactivity of arenes toward nucleophilic aromatic substitution might be closely related to the electron affinity (EA) and lowest unoccupied molecular orbital (LUMO) energies of the substrates. Therefore, we computed these two simple parameters for a series of substituted naphthalenes. As depicted in Figure 2A, the EA (computed as the energy difference between the neutral molecule and its anion with one negative charge) of different 2-substituted naphthalenes was first computed at the B3LYP-D3BJ/6-311+G(d,p)/B3LYP/6–31G(d) level. Substrates with nitrogen substituents such as azo (1.72 eV), nitroso (1.50 eV), and nitro (1.41 eV) groups have the highest EA. We next computed the LUMO energy of these substrates, another great indicator of their reactivity toward nucleophilic aromatic substitution. More importantly, we evaluated the effect of a simple model phosphoric acid (PA) as well by computing the LUMO of the substrate-PA complexes and comparing it with their original LUMO. For example, coordination of PA with 2-nitrosonaphthalene through hydrogen-bond interaction would lower the LUMO energy from 0.85 to 0.42 eV (Figure 2B). Hydrogen-bond interactions between the substrates and PA would presumably lower its LUMO energy and consequently allow for a more facile nucleophilic aromatic substitution to occur. In addition, with CPA catalysts, the stereochemical outcome could be tuned with judicious choice of catalyst scaffolds. The choice of this simple model PA reduced the large conformational space of using more complex CPA catalysts and its associated high computational cost, which allowed us to rapidly screen the effects of different substituents. The screening results are illustrated in Figure 2C, which shows that the nitroso and azo groups are the most promising candidates because of their dramatic decreases in LUMO energy through interactions with PA. The azo group has been verified to be effective for arene functionalization by our recent work.[20] Nitrosoarenes,[27–29] which are widely used in aminoxylation and hydroxyamination reactions with competitive reactive sites on nitrogen and oxygen atoms, proved to be equally promising. However, as far as we know, the site-selective reaction that occurred on the aromatic ring was rarely realized. With these doubts in mind, we initiated the experiment.

Optimizing Reaction Conditions for the Synthesis of Indole-Naphthalene

Axially chiral skeletons are recognized as the core structure of numerous competent ligands or catalysts in asymmetric catalysis for a wide spectrum of useful transformations.[30–33] The unique structural features together with the promising chemical and bioactive properties render the construction of axially chiral scaffolds rewarding yet challenging.[34–56] With 2-nitrosonaphthalene (**1a**) as the promised electrophile, indole (**2a**) was selected as the reaction partner for the asymmetric cross-coupling reaction because of its availability in building atropisomeric molecules. Initially, the reaction of **1a** (0.105 mmol) and **2a** (0.1 mmol) was conducted in CH_2Cl_2 at room temperature (RT) for 1 h under the activation of CPA (*S*)-**C1** (5 mol %). Intriguingly, the expected compound **3a** was not detected, and instead, the oxidation product **4a** was obtained in 12% yield with 62% enantiomeric excess (ee). At the same time, the prevailing nucleophilicity of hydroxylamine yielded compound **5a** containing the axially chiral aniline-indole framework in 18% yield with 65% ee (Table

[1]Shenzhen Grubbs Institute, Department of Chemistry, Southern University of Science and Technology, Shenzhen, Guangdong 518055, China

[2]Department of Chemistry and Biochemistry, University of California, Los Angeles, Los Angeles, CA 90095, USA

[3]Academy for Advanced Interdisciplinary Studies, Southern University of Science and Technology, Shenzhen, Guangdong 518055, China

[4]These authors contributed equally

[5]Lead Contact

*Correspondence: houk@chem.ucla.edu (K.N.H.), tanb@sustech.edu.cn (B.T.)

https://doi.org/10.1016/j.chempr.2020.06.001

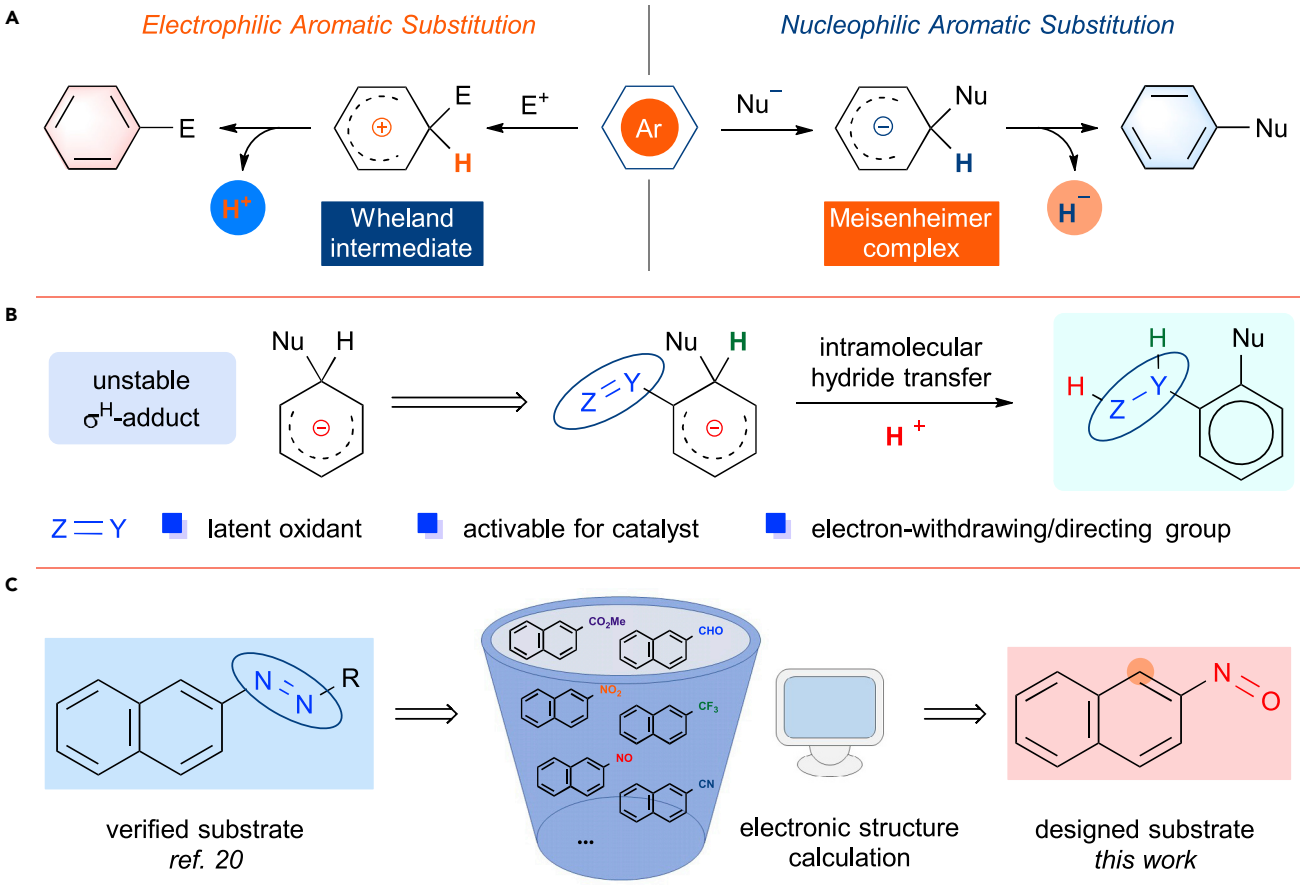

Figure 1. Representative Approaches for Arene Functionalization and Our Design Strategy

(A) Electrophilic aromatic substitution and nucleophilic aromatic substitution via Wheland and Meisenheimer intermediates, respectively.

(B) Our strategy with rapid conversion of the unstable σ^H adduct.

(C) Computational screening for new substrates by electronic structure calculation.

1, entry 1). Despite the convoluted reaction pathway and moderate stereocontrol, these results substantiated the density functional theory (DFT) calculations and our hypothesis. For dominant formation of indole-naphthalene **4a**, an external oxidant was applied with excess **1a** (2.0 equiv), conceding to the oxidability of the nitroso moiety. However, this condition failed to provide a satisfactory outcome (Table 1, entry 2). The aerobic oxidative condition gave similar reaction results (Table 1, entry 3). Delightfully, 81% of **4a** was formed with complete inhibition of product **5a** when quinone was applied as the oxidant (Table 1, entry 4). **C4** was identified as the optimal catalyst in terms of yield and enantioselectivity after a series of CPAs were screened (Table 1, entries 5–12). In addition, an excellent yield (96%) was achieved without ee erosion when modified quinone **O3** was used (Table 1, entry 14). Although further optimization efforts by examining different solvents were futile, it was encouraging to reveal that 1 mol % catalyst loading was sufficient to uphold the high yield and enantioselectivity of this coupling reaction (Table 1, entries 15–18).

Substrate Generality with Respect to Indole-Naphthalene

The generality of the reaction was then examined under the optimized conditions. First, various 2-nitrosonaphthalenes with different substitutions were tested. As depicted in Figure 3A, C6 methoxy-substituted substrate gave the desired product **4b**

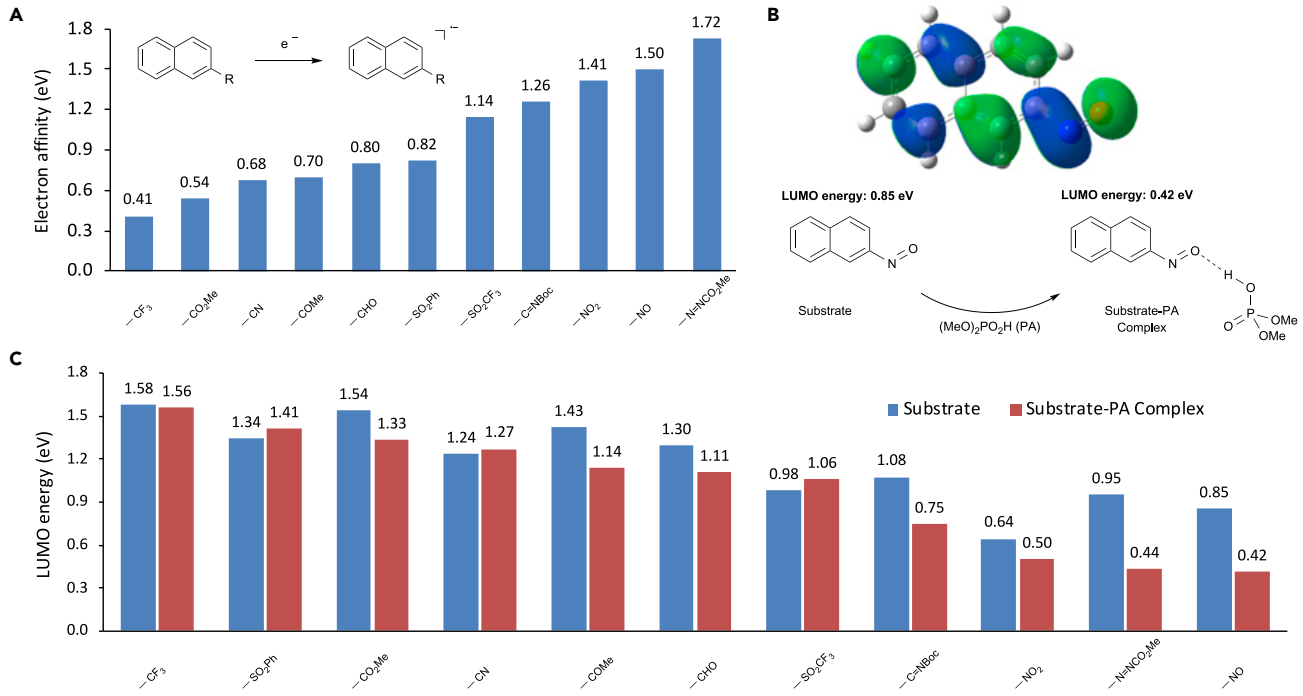

Figure 2. Preliminary Computational Screening of Our Designed Electrophilic Naphthalene Substrates

(A) DFT-computed EA of different substrates.

(B) Illustration of the effect of PA on the LUMO energy of the 2-nitrosonaphthalene substrate.

(C) Computed LUMO energy of the substrates (blue) and of the substrate-PA complexes (red).

in excellent yield with up to 99% ee. The yield declined slightly to 88% (**4c**) when a methyl group was installed in place of the methoxy group. Phenyl, benzoyloxy, amine, and pyrrolyl groups were well tolerated for this reaction to give the corresponding products in excellent yields and enantioselectivities (**4d**, **4e**, and **4h–4j**), whereas moderate yields were obtained for substrates with C6 electron-withdrawing groups (**4f** and **4g**), which might be ascribed to the poor solubility of the substrates (**1f** and **1g**) in CH_2Cl_2. Excellent yields and enantioselectivities were obtained when the substituents were equipped at the C7 position of **1a** (**4k–4m**). Further substrate exploration illustrated that all examined indoles with diverse substituents at varied positions underwent smooth transformations to produce the desired atropisomers **4n–4u** in excellent enantiocontrol (Figure 3B). Aside from the *tert*-butyl group, the *tert*-pentyl and 1-adamantyl groups could also effect restricted rotation of the stereogenic axis (**4v** and **4w**), whereas the phenyl, isopropyl, and methyl-substituted cyclopropyl moieties posing less steric hindrance were found to be invalid axial-rotation restriction groups; meanwhile, the atropisomerism of the corresponding products (**4x–4z**) lost rapidly even at RT in the reaction mixture. To enhance the stability of the stereogenic axis, a methyl group was introduced at the C4 position of 2-phenylindole **2n**. Even though 72% ee was obtained for the expected **4aa** under the developed conditions, the configurational stability was clearly confirmed. The re-evaluation of CPAs proved (*S*)-**C20** as the other promising catalyst for this type of substrate because it furnished atropisomer **4aa** in 55% yield with a satisfied enantiocontrol (86% ee). It should be mentioned that 5 mol % catalyst loading and 16 h reaction time were required because of the probably low reactivity of **2aa** with C4 substitution (Table S3). A similar reaction outcome was found for the preparation of **4ab**, whereas **C4** was verified to be a better catalyst for assembling indole-naphthalene **4ac** in terms of enantioselectivity. Interestingly, a small methyl group at the C2

Table 1. Optimization of the Reaction Conditions for Indole-Naphthalene 4a

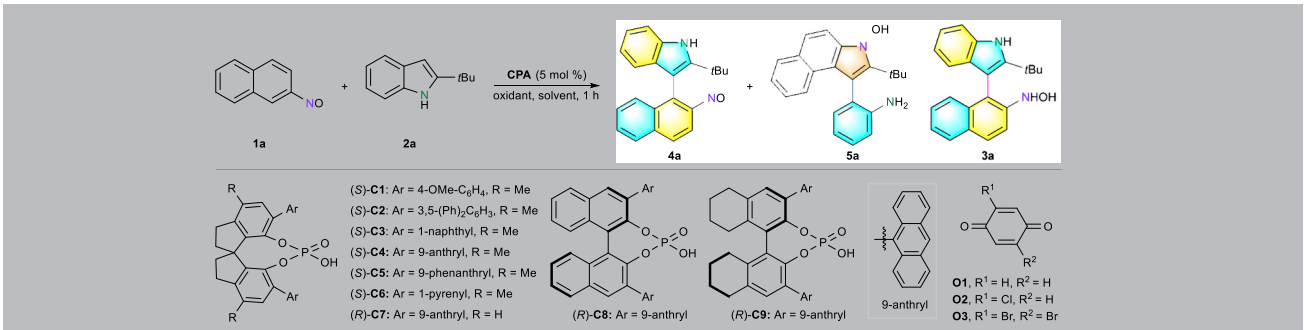

Entry[a]	Solvent	CPA	Oxidant	4a		5a	
				Yield (%)[b]	ee (%)[c]	Yield (%)[b]	ee (%)[c]
1	CH_2Cl_2	(*S*)-C1	none	12	62	18	65
2	CH_2Cl_2	(*S*)-C1	excess **1a**	21	55	36	53
3	CH_2Cl_2	(*S*)-C1	O_2	12	59	15	60
4	CH_2Cl_2	(*S*)-C1	O1	81	64	trace	–
5	CH_2Cl_2	(*S*)-C2	O1	75	86	–	–
6	CH_2Cl_2	(*S*)-C3	O1	84	87	–	–
7	CH_2Cl_2	(*S*)-C4	O1	87	96	–	–
8	CH_2Cl_2	(*S*)-C5	O1	84	96	–	–
9	CH_2Cl_2	(*S*)-C6	O1	81	94	–	–
10	CH_2Cl_2	(*R*)-C7	O1	87	−96	–	–
11	CH_2Cl_2	(*R*)-C8	O1	82	57	–	–
12	CH_2Cl_2	(*R*)-C9	O1	79	28	–	–
13	CH_2Cl_2	(*S*)-C4	O2	63	94	–	–
14	CH_2Cl_2	(*S*)-C4	O3	96	96	–	–
15	$CHCl_3$	(*S*)-C4	O3	81	85	–	–
16	toluene	(*S*)-C4	O3	90	95	–	–
17	EtOAc	(*S*)-C4	O3	93	76	–	–
18[d]	CH_2Cl_2	(*S*)-C4	O3	96	96	–	–

[a]Unless otherwise stated, all reactions were carried out with **1a** (0.105 mol), **2a** (0.1 mmol), oxidant (0.11 mmol), and CPA (5 mol %) in 4 mL of solvent at RT for 1 h.
[b]Isolated yields were provided.
[c]The enantiomeric excess (ee) values were determined by chiral HPLC analysis.
[d]Using 1 mol % of CPA, 3 h.

position could effectively lock the stereogenic axis with the assistance of C4 methyl substitution. By contrast, no good results were obtained for the substrates with a bulky C2 substituent, such as isopropyl or methyl-substituted cyclopropyl, for both catalysts because of the low activity. The absolute configuration of **4u** was determined by X-ray crystallographic analysis after recrystallization, and those of other products in Figure 3 were assigned by analogy. Furthermore, the practicality of this asymmetric cross-coupling reaction was verified by a gram-scale reaction between **1a** and **2a** with negligible yield and enantioselectivity variation.

Optimizing Reaction Conditions for the Synthesis of Aniline-Indole

Having secured the enantioselective construction of atropisomeric indole-naphthalene scaffold, we moved on to selectively synthesize axially chiral aniline-indole **5**.

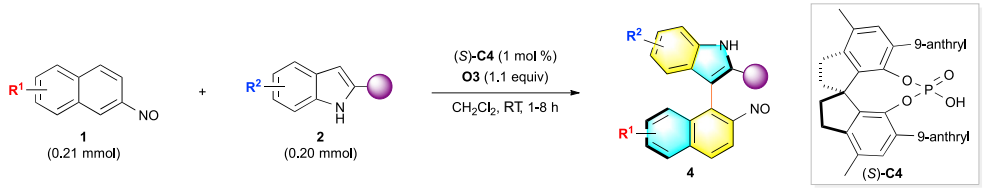

A : Substrate scope of 2-nitrosonaphthalenes

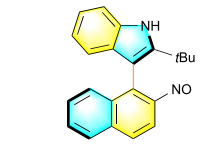
4a, 96% yield, 96% ee
Gram-scale: 94% yield, 96% ee

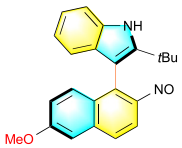
4b, 90% yield, 99% ee

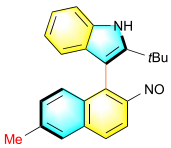
4c, 88% yield, 97% ee

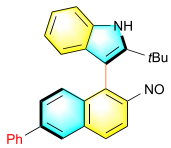
4d, 91% yield, 99% ee

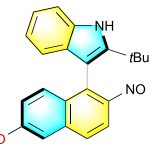
4e, 90% yield, 98% ee

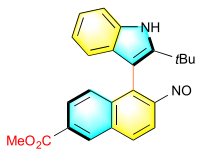
4f, 64% yield, 97% ee

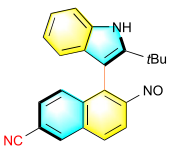
4g, 68% yield, 96% ee

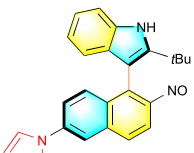
4h, 89% yield, 98% ee

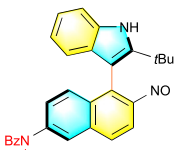
4i, 91% yield, 95% ee

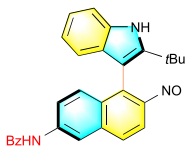
4j, 88% yield, 97% ee

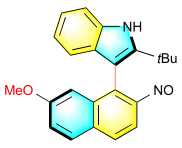
4k, 92% yield, 97% ee

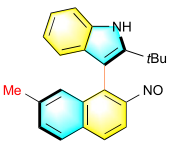
4l, 94% yield, 97% ee

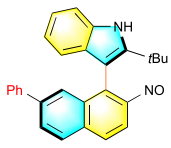
4m, 93% yield, 97% ee

B : Substrate scope of indoles

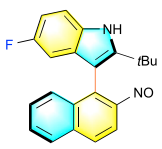
4n, 93% yield, 97% ee

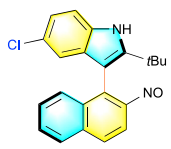
4o, 97% yield, 97% ee

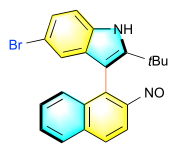
4p, 96% yield, 98% ee

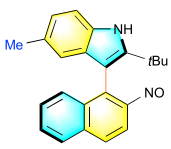
4q, 89% yield, 99% ee

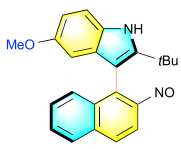
4r, 93% yield, 98% ee

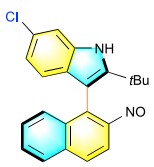
4s, 95% yield, 98% ee

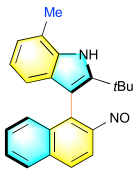
4t, 84% yield, 98% ee

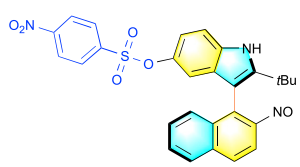
4u, 96% yield, 98% ee

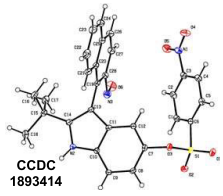
CCDC
1893414

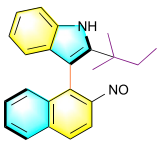
4v, 94% yield, 97% ee

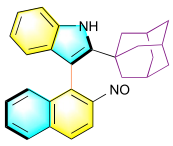
4w, 69% yield, 91% ee

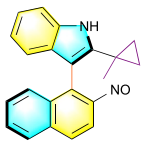
4x, 91% yield[a]

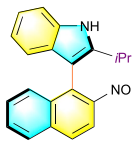
4y, 96% yield[a]

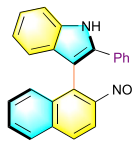
4z, 75% yield[a]

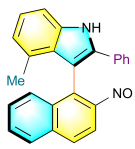
4aa[b]
(*S*)-**C20**: 55%, 86% ee

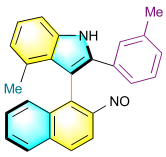
4ab[b]
(*S*)-**C20**: 53%, 87% ee

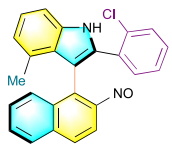
4ac[b]
61%, 92% ee

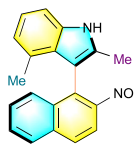
4ad
70%, 83% ee

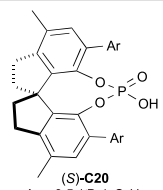
(*S*)-**C20**
Ar = 3,5-(*t*Bu)$_2$C$_6$H$_3$

Figure 3. Substrate Generality for Indole-Naphthalene 4

Reaction conditions: **1** (0.21 mmol), **2** (0.20 mmol), **O3** (1.1 equiv), and (*S*)-**C4** (1 mol %) in CH_2Cl_2 (8 mL) at RT for 1–8 h.

(A) Substrate scope of 2-nitrosonaphthalenes.

(B) Substrate scope of indoles and X-ray structure of compound **4u**.

[a]Rapid racemization in the reaction mixture.

[b]5 mol % catalyst loading for 16 h.

The optimal catalyst (*S*-**C4**) and solvent (CH_2Cl_2) were used for the reaction of **1a** and **2a** at RT in the absence of an external oxidant. Under this set of conditions, dominant formation of **5a** (48%) was achieved as expected, although formation of **4a** (11%) and recovery of **2a** (34%) were also unequivocal (Table 2, entry 1). Subsequently, solvent screening uncovered that ethyl acetate (EtOAc) was superior for this transformation in light of the overall reaction outcome (Table 2, entries 2–5). Detailed evaluation of numerous CPAs suggested that the catalytic activity of **C4** was unparalleled (Table 2, entries 6–13). Further optimizations also disclosed that increased loading of **1a** (2.0 equiv) and lower reaction concentration could improve the isolated yield of **5a** to 76% with 99% ee (Table 2, entry 14).

Substrate Generality with Respect to Aniline-Indole

The modified conditions were then applied to a wide range of 2-nitrosonaphthalenes and indoles. As depicted in Figure 4A, coupling partner **1** bearing a methyl, methoxy, or phenyl group at the C6 or C7 position was efficacious for this reaction to furnish desired products with remarkable stereocontrol (**5b–5g**). However, the introduction of strong electron-donating methoxy group on 2-nitrosonaphthalene (**1b** and **1k**) significantly increased the formation of the byproduct (**4b** and **4k**) and gave rise to the low yield of the corresponding product (**5d** and **5e**). Meanwhile, the poor solubility of the substrates bearing an electron-withdrawing functionality in EtOAc led to a conspicuous decrement in conversion rate and yield (**5h–5j**). On the contrary, the alteration on the indole ring, including a different substitution pattern (**5n–5t**), as well as the axial rotation resistance group (**5u–5w**), brought about an inconspicuous yield variation (Figure 4B). Notably, current conditions were also well accommodated by halogenated indoles, such as fluoride, chloride, and bromide. Moreover, all investigated substrates furnished respective aniline-indole atropisomers with up to 99% ee. The absolute configuration of **5k** was determined by X-ray crystallographic analysis after recrystallization, and those of other products in Figure 4 were assigned by analogy.

Reaction Mechanism and Computational Study

On the basis of experimental results and our understanding of organocatalytic asymmetric construction of atropisomeric structures, a plausible reaction pathway was proposed (Figure 5A). The reaction is initiated with an enantioselective nucleophilic attack of indole to 2-nitrosonaphthalene to generate intermediate **A** through rapid intramolecular conversion of the unstabilized σ^H adduct mediated by bifunctional CPA catalysis. The re-aromatization process thus produces unstable intermediate **B**. After an intramolecular cyclization induced by the highly nucleophilic hydroxylamine moiety, the ensuing β-H elimination and C–N bond cleavage form axially chiral indole-aniline **5a** dominantly. Atropisomeric indole-naphthalene structure **4a** is exclusively generated instead in the presence of an external oxidant. We also computed the transition states (TSs) for the first step (C–C bond forming) of this transformation. The two lowest-energy-transition structures for this CPA-catalyzed asymmetric nucleophilic attack are shown in Figure 5B. In each of the two TSs, the C–C bond is being formed, whereas the proton is almost completely transferred from the CPA to the nitroso oxygen. Simultaneously, the Brønsted basic site of the CPA coordinates to the N–H of the indole through a hydrogen bond. Overall, the CPA acts as a bifunctional catalyst to promote this key C–C bond formation. The

Table 2. Optimization of the Reaction Conditions for Aniline-Indole 5a

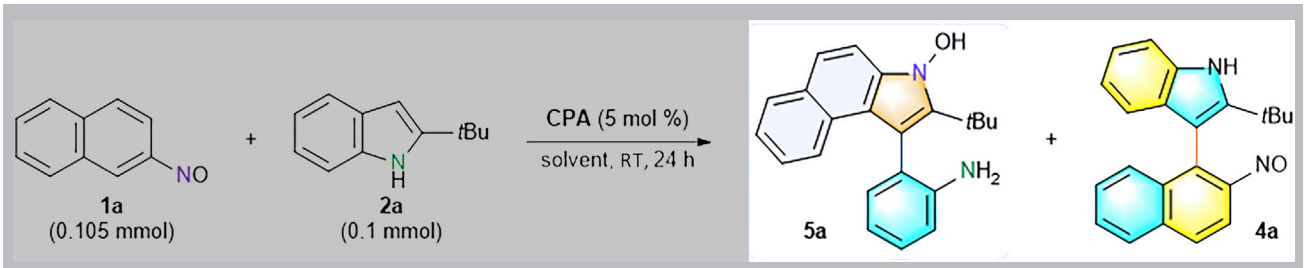

Entry[a]	CPA	Solvent	Yield (%)		ee (%)[b]	
			5a[c]	4a[d]	5a	4a
1	(*S*)-C4	CH_2Cl_2	48	11	98	96
2	(*S*)-C4	CCl_4	36	7	98	96
3	(*S*)-C4	EtOAc	57	6	99	96
4	(*S*)-C4	toluene	45	7	98	95
5	(*S*)-C4	*c*-hexane	18	1	95	88
6	(*S*)-C1	EtOAc	15	16	22	19
7	(*S*)-C2	EtOAc	27	11	79	61
8	(*S*)-C3	EtOAc	33	10	90	81
9	(*S*)-C5	EtOAc	51	6	96	83
10	(*S*)-C6	EtOAc	43	9	95	83
11	(*R*)-C7	EtOAc	51	6	−99	−95
12	(*R*)-C8	EtOAc	30	16	63	61
13	(*R*)-C9	EtOAc	24	14	63	65
14[e]	(*S*)-C4	EtOAc	76	5	99	94

[a]Unless otherwise stated, all reactions were carried out with **1a** (0.105 mmol), **2a** (0.1 mmol), and CPA (5 mol %) in 5 mL of solvent at RT for 24 h under argon atmosphere.
[b]The enantiomeric excess (ee) values were determined by chiral HPLC analysis.
[c]Isolated yields were provided.
[d]The yields were determined by ^{1}H NMR analysis of the crude product.
[e]Using **1a** (0.4 mmol), **2a** (0.2 mmol), and EtOAc (8 mL), 24 h.

lowest-energy TS (TS-major) that ultimately leads to the major atropisomeric product is 2.2 kcal mol^{-1} more stable than TS-minor. In TS-major, the C–N bond of the 2-nitrosonaphthalene substrate adopts the more stable *s-trans* conformation (1.4 kcal mol^{-1} more stable), whereas it is *s-cis* in TS-minor (the *s-trans* conformation results in a poorer fit in the catalyst pocket). In addition, we calculated the distortion energy and found that the catalyst itself is 0.8 kcal mol^{-1} more distorted in TS-minor. In TS-major, one dihedral angle (−64.1°) between the anthryl group and the backbone of the catalyst rotates away from the ideal −68.0° geometry,[57] whereas the other dihedral angle is perfectly preserved (−68.2°). In contrast, both dihedral angles in TS-minor rotate away from ideal, causing a slightly higher distortion energy in the catalyst. These two factors lead to the 2.2 kcal mol^{-1} difference in energy between the two TSs, which explains the observed enantioselectivity of this reaction. A diagram of the reaction free energy is shown in Figure 5C. After the formation of the C–C bond and the subsequent aromatization of the naphthalene ring, **II** is generated. In the absence of an external oxidant, an intramolecular cyclization proceeds to form **III** (Figure 5C, red pathway), as induced by the highly nucleophilic hydroxylamine moiety. Subsequent C–N bond cleavage forms **Int. 5**, which undergoes β-H elimination to generate **Int. 6** (the axially chiral indole-aniline **5a** in complex with the CPA). In

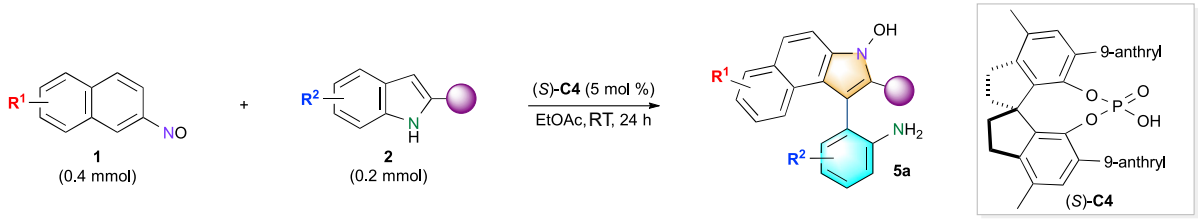

A: Substrate scope of 2-nitrosonaphthalenes

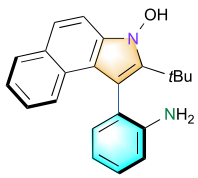

5a, 76% yield, 99% ee

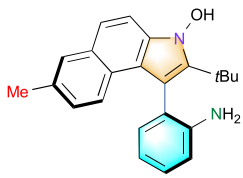

5b, 77% yield, 97% ee

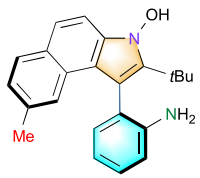

5c, 79% yield, 98% ee

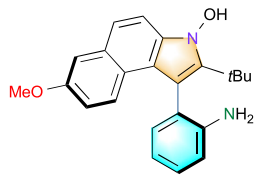

5d, 51% yield, 98% ee

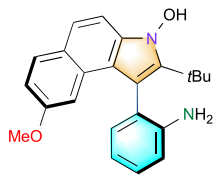

5e, 60% yield, 99% ee

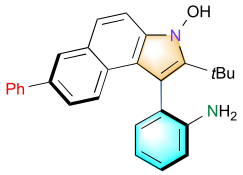

5f, 65% yield, 99% ee

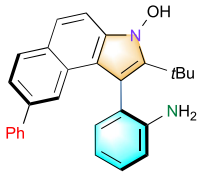

5g, 71% yield, 99% ee

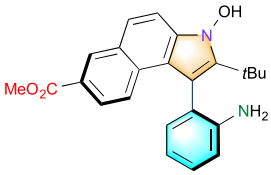

5h, 59% yield, 99% ee

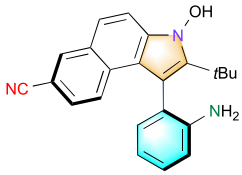

5i, 61% yield, 98% ee

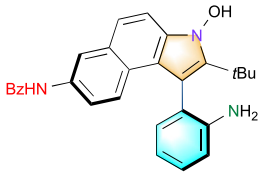

5j, 57% yield, 99% ee[a]

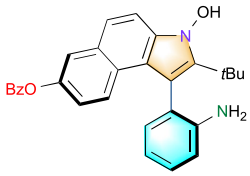

5k, 72% yield, 99% ee

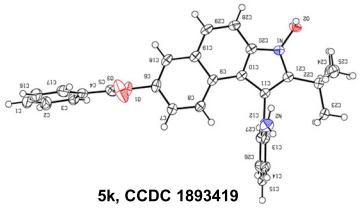

5k, CCDC 1893419

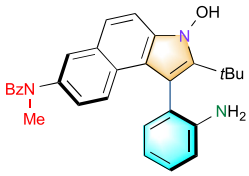

5l, 70% yield, 99% ee

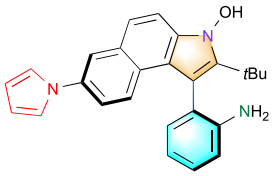

5m, 73% yield, 99% ee

B: Substrate scope of indoles

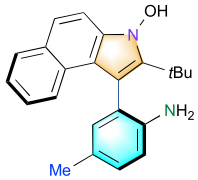

5n, 71% yield, 99% ee

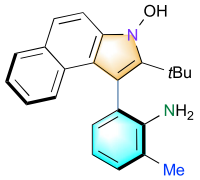

5o, 76% yield, 99% ee

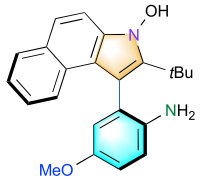

5p, 72% yield, 99% ee

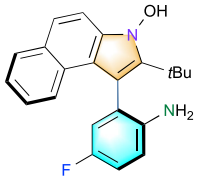

5q, 65% yield, 98% ee

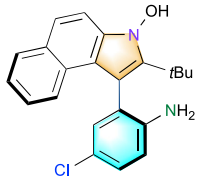

5r, 71% yield, 98% ee

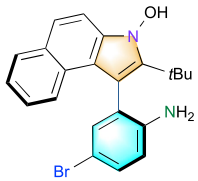

5s, 72% yield, 98% ee

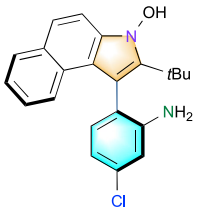

5t, 78% yield, 99% ee

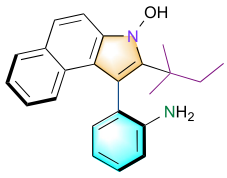

5u, 72% yield, 99% ee

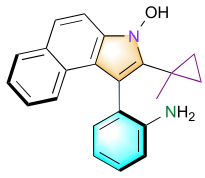

5v, 77% yield, 95% ee

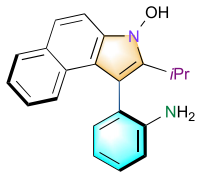

5w, 76% yield, 96% ee

Figure 4. Substrate Generality for Aniline-Indole 5

Reaction conditions: **1** (0.4 mmol), **2** (0.2 mmol), and (*S*)-**C4** (5 mol %) in EtOAc (8 mL) for 24 h under argon atmosphere.

(A) Substrate scope of 2-nitrosonaphthalenes and X-ray structure of compound **5k**.

(B) Substrate scope of indoles.

[a]12 mL of EtOAc was used.

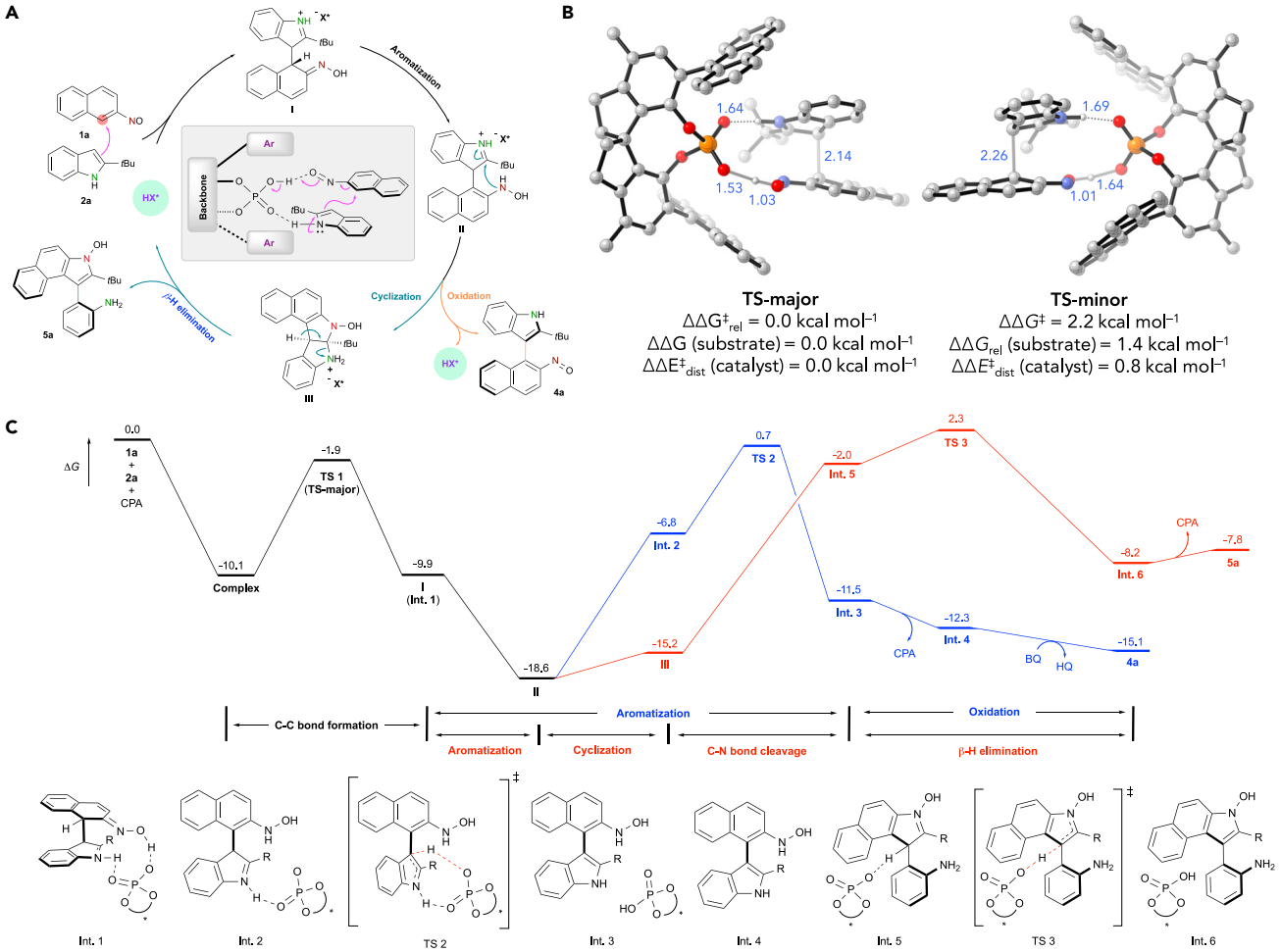

Figure 5. Reaction Mechanisms

(A) Proposed mechanism for the CPA-catalyzed asymmetric nitrosonaphthalene functionalization and rearrangement.

(B) DFT-computed stereo-determining transition structures.

(C) Diagram of the computed reaction free energy.

R, tBu; CPA, (*S*)-**C4**; BQ, benzoquinone; HQ, hydroquinone.

the presence of an external oxidant, such as benzoquinone, further aromatization of II generates **Int. 4**, which could be oxidized to form product **4a** (Figure 5C, blue pathway). More computed mechanistic details can be found in Figures S2 and S3.

Asymmetric Construction of NOBIN Structures

Successful establishment of the highly enantioselective construction of indole-naphthalene and indole-aniline analogs inspired us to explore the feasibility of constructing privileged axially chiral scaffolds. The NOBIN (2-amino-2′-hydroxy-1,1′-binaphthyl) structure is present in a multitude of highly prized biaryl atropisomeric catalysts and ligands for chirality induction in asymmetric catalysis.[58,59] However, the catalytic asymmetric construction approaches are scarce, thus restricting their applications.[60,61] In particular, a facile and universal organocatalytic protocol remains hitherto inaccessible. As a result of the unmet challenge in the assembly of atropisomeric NOBINs, the aforementioned strategy was then extended to 2-naphthol nucleophile. Compared with indole, this reaction was assumed to be more challenging and complicated because of the disparate nucleophilicity and the multiple

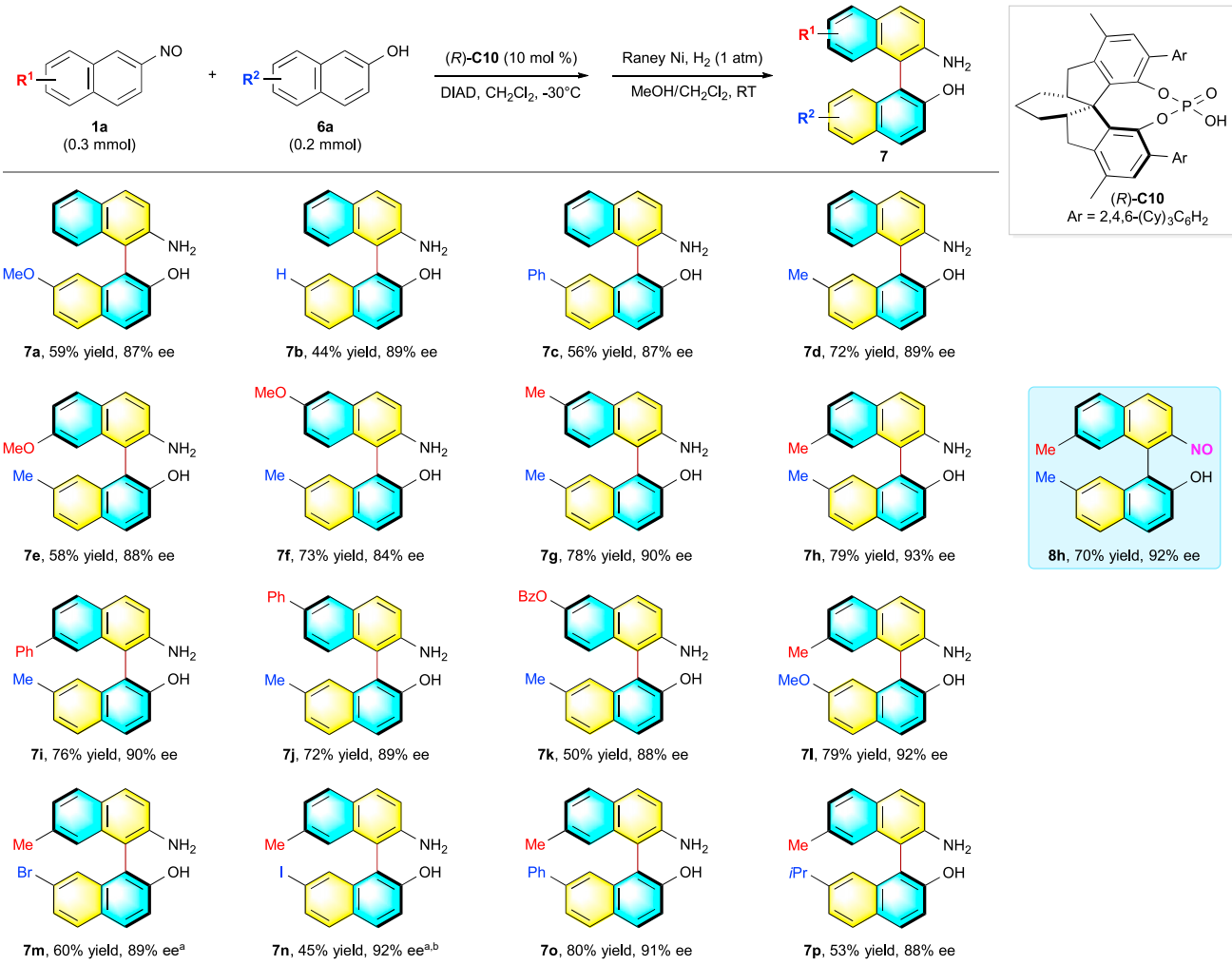

Figure 6. Substrate Generality for NOBINs 7 and the Isolation of Intermediate 8h

Reaction conditions: **1** (0.3 mol), **6** (0.2 mmol), DIAD (0.2 mmol), and (*R*)-**C10** (10 mol %) in CH_2Cl_2 (4 mL) at −30°C for 2 days; reaction mixture of the first step and Raney-Ni (50 mg) in MeOH (4 mL) under H_2 atmosphere (1 atm) for 1 h.

[a]Zinc powder and HCO_2H were used as the reductant.

[b]CH_2Cl_2 (6 mL) for the first step.

reactive sites present. Nonetheless, an array of valuable NOBINs were auspiciously fashioned with remarkable enantiocontrol through a one-pot, two-step synthesis, namely asymmetric C–C cross-coupling and reductive N–O bond cleavage. Notably, CPA (*R*)-**C10** with a cyclohexyl-fused spirobiindane backbone[62] was found to be the best catalyst, and the addition of diisopropyl azodicarboxylate (DIAD) as an oxidant could significantly boost the yield (Tables S1 and S2). The generality and limitation of this reaction are depicted in Figure 6. First, the model reaction with C7 methoxy-substituted 2-naphthol afforded the desired **7a** in 59% yield with 87% ee in CH_2Cl_2 at −30°C for 2 days. Subsequent evaluation demonstrated that the substitution on the C7 position of 2-naphthol strongly influenced the reaction results (**7b–7d**). Pleasingly, the yield was improved to 72% when a methyl group was introduced (**7d**). We next examined the substitution effect on 2-nitrosonaphthalene with **6d** as the coupling partner, and the results further proved the positive impact of C7 methyl substitution on 2-naphthol (**7e–7k**). In addition, the installation of a methyl group on the C7 position of 2-nitrosonaphthalene could contribute to the enantiocontrol of atroposelective

cross-coupling reactions (**7h** and **7l–7p**). Delightfully, the isolation of enantioenriched 2-hydroxy-2′-nitroso-binaphthyl **8h** clearly indicated a reaction pathway similar to that presented in Figure 5A and the oxidation effect of DIAD. Comparison of the chiral high-performance liquid chromatography (HPLC) spectrum of synthesized **7b** with that of commercially available (*S*)-NOBIN determined the absolute configuration of **7b** to be (*S*). Those of other products **7** and **8h** were assigned analogously.

An efficient organocatalytic arene functionalization strategy with 2-nitrosonaphthalene as the electrophile was efficiently developed, guided by DFT calculations. The nitroso group could serve as a directing electron-withdrawing group and an oxidant for rapid conversion of the unstabilized σ^H adduct. The atroposelective nucleophilic aromatic substitution reactions were realized under mild reaction conditions enabled by CPA catalysis, generating two types of highly enantioenriched atropisomers (indole-naphthalenes and indole-anilines) encompassing a wide substrate scope. Employing a CPA with a cyclohexyl-fused spirobiindane backbone, we further demonstrated the practicality of this strategy by applying a one-pot, two-step synthesis of privileged axially chiral NOBIN and its derivatives. Compared with the previously disclosed azo group,[20,60] a nitroso group effectively negates the necessity of an appending electron-withdrawing ester functionality. Accordingly, the atom economy of the current approach was significantly improved. Meanwhile, the high reactivity of the 2-nitrosonaphthalene authorized a solo organocatalytic system that aptly realized the asymmetric construction of NOBINs, thus signifying another graceful departure from a more reactive and complex catalytic species required to facilitate analogous transformation of azo-embedded arene substrates. DFT calculations provide additional insights into the origins of enantiocontrol.

EXPERIMENTAL PROCEDURES

Full experimental procedures are provided in the Supplemental Information.

Resource Availability

Lead Contact

Further information and requests for resources should be directed to and will be fulfilled by the Lead Contact, Bin Tan (tanb@sustech.edu.cn).

Materials Availability

This study did not generate new unique reagents.

Data and Code Availability

The X-ray crystallographic coordinates for the structures of **4u** and **5k** reported in this article have been deposited at the Cambridge Crystallographic Data Centre (CCDC) under accession numbers CCDC: 1893414 and CCDC: 1893419. These data can be obtained free of charge from CCDC via http://www.ccdc.cam.ac.uk/data_request/cif. Experimental procedures and characterization of new compounds are available in the Supplemental Information.

SUPPLEMENTAL INFORMATION

Supplemental Information can be found online at https://doi.org/10.1016/j.chempr.2020.06.001.

ACKNOWLEDGMENTS

We are grateful for financial support from the National Natural Science Foundation of China (21772081, 21825105, 21702092, and 21901105), the Shenzhen Nobel

Prize Scientists Laboratory Project (C17213101), Shenzhen Special Funds (JCYJ20180305123508258), and the US National Science Foundation (CHE-1764328) and Saul Winstein Chair in Organic Chemistry funds to K.N.H. Computational work was supported by the Center for Computational Science and Engineering at SUSTech and by the UCLA Institute of Digital Research and Education.

AUTHOR CONTRIBUTIONS

B.T. and K.N.H. conceived and directed the project; W.-Y.D. and Q.-J.A. designed and performed experiments; P.Y. and K.L.B. conducted the DFT calculations and provided mechanism analysis; S.-H.X., S.L., and Y.C. helped with the collection of some new compounds and data analysis; B.T., K.N.H., S.-H.X., and P.Y. wrote the paper with input from all other authors; and all authors discussed the results and commented on the manuscript. W.-Y.D., P.Y., Q.-J.A., and K.L.B. contributed equally to this work.

DECLARATION OF INTERESTS

The authors declare no competing interests.

Received: February 6, 2020
Revised: April 20, 2020
Accepted: May 29, 2020
Published: June 23, 2020

REFERENCES

1. Mortier, J. (2015). Arene Chemistry: Reaction Mechanism and Methods for Aromatic Compounds (John Wiley & Sons).
2. Friedel, C., and Crafts, J.-M. (1877). Sur une nouvelle méthode générale de synthèse d'hydrocarbures, d'acétones, etc. C. R. Chim. *84*, 1392–1395.
3. Sartori, G., and Maggi, R. (2017). Advance in Friedel-Crafts Acylation Reactions: Catalytic and Green Processes (CRC Press).
4. Bandini, M., and Umani-Ronchi, A. (2009). Catalytic Asymmetric Friedel-Crafts Alkylations (John Wiley & Sons).
5. Daugulis, O., Do, H.Q., and Shabashov, D. (2009). Palladium- and copper-catalyzed arylation of carbon-hydrogen bonds. Acc. Chem. Res. *42*, 1074–1086.
6. Colby, D.A., Bergman, R.G., and Ellman, J.A. (2010). Rhodium-catalyzed C–C bond formation via heteroatom-directed C–H bond activation. Chem. Rev. *110*, 624–655.
7. Lyons, T.W., and Sanford, M.S. (2010). Palladium-catalyzed ligand-directed C-H functionalization reactions. Chem. Rev. *110*, 1147–1169.
8. Wencel-Delord, J., Dröge, T., Liu, F., and Glorius, F. (2011). Towards mild metal-catalyzed C-H bond activation. Chem. Soc. Rev. *40*, 4740–4761.
9. Engle, K.M., Mei, T.S., Wasa, M., and Yu, J.Q. (2012). Weak coordination as a powerful means for developing broadly useful C-H functionalization reactions. Acc. Chem. Res. *45*, 788–802.
10. Wang, P., Verma, P., Xia, G., Shi, J., Qiao, J.X., Tao, S., Cheng, P.T.W., Poss, M.A., Farmer, M.E., Yeung, K.S., and Yu, J.-.Q. (2017). Ligand-accelerated non-directed C–H functionalization of arenes. Nature *551*, 489–493.
11. Romero, N.A., Margrey, K.A., Tay, N.E., and Nicewicz, D.A. (2015). Site-selective arene C-H amination via photoredox catalysis. Science *349*, 1326–1330.
12. Mąkosza, M. (2010). Nucleophilic substitution of hydrogen in electron-deficient arenes, a general process of great practical value. Chem. Soc. Rev. *39*, 2855–2868.
13. Mąkosza, M. (2014). Reactions of nucleophiles with nitroarenes: multifacial and versatile electrophiles. Chemistry *20*, 5536–5545.
14. Wilson, A.S.S., Hill, M.S., Mahon, M.F., Dinoi, C., and Maron, L. (2017). Organocalcium-mediated nucleophilic alkylation of benzene. Science *358*, 1168–1171.
15. Mąkosza, M., and Winiarski, J. (1987). Vicarious nucleophilic substitution of hydrogen. Acc. Chem. Res. *20*, 282–289.
16. Houk, K.N., and List, B. (2004). Asymmetric organocatalysis. Acc. Chem. Res. *37*, 487.
17. List, B. (2007). Introduction: organocatalysis. Chem. Rev. *107*, 5413–5415.
18. MacMillan, D.W.C. (2008). The advent and development of organocatalysis. Nature *455*, 304–308.
19. B. List, ed. (2010). Asymmetric Organocatalysis (Springer). https://doi.org/10.1007/978-3-642-02815-1.
20. Qi, L.W., Mao, J.H., Zhang, J., and Tan, B. (2018). Organocatalytic asymmetric arylation of indoles enabled by azo groups. Nat. Chem. *10*, 58–64.
21. Akiyama, T. (2007). Stronger Brønsted acids. Chem. Rev. *107*, 5744–5758.
22. Terada, M. (2008). Binaphthol-derived phosphoric acid as a versatile catalyst for enantioselective carbon-carbon bond forming reactions. Chem. Commun. *2008*, 4097–4112.
23. Parmar, D., Sugiono, E., Raja, S., and Rueping, M. (2014). Complete field guide to asymmetric BINOL-phosphate derived Brønsted acid and metal catalysis: history and classification by mode of activation; Brønsted acidity, hydrogen bonding, ion pairing, and metal phosphates. Chem. Rev. *114*, 9047–9153.
24. Bella, M., Kobbelgaard, S., and Jørgensen, K.A. (2005). Organocatalytic regio- and asymmetric *C*-selective S_NAr reactions-stereoselective synthesis of optically active spiro-pyrrolidone-3,3′-oxoindoles. J. Am. Chem. Soc. *127*, 3670–3671.
25. Shirakawa, S., Koga, K., Tokuda, T., Yamamoto, K., and Maruoka, K. (2014). Catalytic asymmetric synthesis of 3,3′-diaryloxindoles as triarylmethanes with a chiral all-carbon quaternary center: phase-transfer-catalyzed S_NAr reaction. Angew. Chem. Int. Ed. *53*, 6220–6223.
26. Armstrong, R.J., and Smith, M.D. (2014). Catalytic enantioselective synthesis of atropisomeric biaryls: a cation-directed nucleophilic aromatic substitution reaction. Angew. Chem. Int. Ed. *53*, 12822–12826.

27. Zhong, G.-F. (2003). A facile and rapid route to highly enantiopure 1,2-diols by novel catalytic asymmetric α-aminoxylation of aldehydes. Angew. Chem. Int. Ed. *42*, 4247–4250.

28. Brown, S.P., Brochu, M.P., Sinz, C.J., and MacMillan, D.W.C. (2003). The direct and enantioselective organocatalytic α-oxidation of aldehydes. J. Am. Chem. Soc. *125*, 10808–10809.

29. Lu, M., Zhu, D., Lu, Y., Zeng, X., Tan, B., Xu, Z., and Zhong, G. (2009). Chiral Brønsted acid-catalyzed enantioselective α-hydroxylation of β-dicarbonyl compounds. J. Am. Chem. Soc. *131*, 4562–4563.

30. Noyori, R., and Takaya, H. (1990). BINAP: an efficient chiral element for asymmetric catalysis. Acc. Chem. Res. *23*, 345–350.

31. Chen, Y., Yekta, S., and Yudin, A.K. (2003). Modified BINOL ligands in asymmetric catalysis. Chem. Rev. *103*, 3155–3212.

32. Brunel, J.M. (2005). BINOL: a versatile chiral reagent. Chem. Rev. *105*, 857–897.

33. Berthod, M., Mignani, G., Woodward, G., and Lemaire, M. (2005). Modified BINAP: the how and the why. Chem. Rev. *105*, 1801–1836.

34. Kozlowski, M.C., Morgan, B.J., and Linton, E.C. (2009). Total synthesis of chiral biaryl natural products by asymmetric biaryl coupling. Chem. Soc. Rev. *38*, 3193–3207.

35. Gustafson, J.L., Lim, D., and Miller, S.J. (2010). Dynamic kinetic resolution of biaryl atropisomers via peptide-catalyzed asymmetric bromination. Science *328*, 1251–1255.

36. Mori, K., Ichikawa, Y., Kobayashi, M., Shibata, Y., Yamanaka, M., and Akiyama, T. (2013). Enantioselective synthesis of multisubstituted biaryl skeleton by chiral phosphoric acid catalyzed desymmetrization/kinetic resolution sequence. J. Am. Chem. Soc. *135*, 3964–3970.

37. Barrett, K.T., Metrano, A.J., Rablen, P.R., and Miller, S.J. (2014). Spontaneous transfer of chirality in an atropisomerically enriched two-axis system. Nature *509*, 71–75.

38. Kumarasamy, E., Raghunathan, R., Sibi, M.P., and Sivaguru, J. (2015). Nonbiaryl and heterobiaryl atropisomers: molecular templates with promise for atropselective chemical transformations. Chem. Rev. *115*, 11239–11300.

39. Wencel-Delord, J., Panossian, A., Leroux, F.R., and Colobert, F. (2015). Recent advances and new concepts for the synthesis of axially stereoenriched biaryls. Chem. Soc. Rev. *44*, 3418–3430.

40. Wang, Y.B., and Tan, B. (2018). Construction of axially chiral compounds via asymmetric organocatalysis. Acc. Chem. Res. *51*, 534–547.

41. Wang, J.Z., Zhou, J., Xu, C., Sun, H., Kürti, L., and Xu, Q.L. (2016). Symmetry in cascade chirality-transfer processes: a catalytic atroposelective direct arylation approach to BINOL derivatives. J. Am. Chem. Soc. *138*, 5202–5205.

42. Quinonero, O., Jean, M., Vanthuyne, N., Roussel, C., Bonne, D., Constantieux, T., Bressy, C., Bugaut, X., and Rodriguez, J. (2016). Combining organocatalysis with central-to-axial chirality conversion: atroposelective Hantzsch-type synthesis of 4-arylpyridines. Angew. Chem. Int. Ed. *55*, 1401–1405.

43. Raut, V.S., Jean, M., Vanthuyne, N., Roussel, C., Constantieux, T., Bressy, C., Bugaut, X., Bonne, D., and Rodriguez, J. (2017). Enantioselective syntheses of furan atropisomers by an oxidative central-to-axial chirality conversion strategy. J. Am. Chem. Soc. *139*, 2140–2143.

44. Zhang, H.H., Wang, C.S., Li, C., Mei, G.J., Li, Y., and Shi, F. (2017). Design and enantioselective construction of axially chiral naphthyl-indole skeletons. Angew. Chem. Int. Ed. *56*, 116–121.

45. Jolliffe, J.D., Armstrong, R.J., and Smith, M.D. (2017). Catalytic enantioselective synthesis of atropisomeric biaryls by a cation-directed O-alkylation. Nat. Chem. *9*, 558–562.

46. Zhao, K., Duan, L., Xu, S., Jiang, J., Fu, Y., and Gu, Z. (2018). Enhanced reactivity by torsional strain of cyclic diaryliodonium in Cu-catalyzed enantioselective ring-opening reaction. Chem *4*, 599–612.

47. Hornillos, V., Carmona, J.A., Ros, A., Iglesias-Sigüenza, J., López-Serrano, J., Fernández, R., and Lassaletta, J.M. (2018). Dynamic kinetic resolution of heterobiaryl ketones by zinc-catalyzed asymmetric hydrosilylation. Angew. Chem. Int. Ed. *57*, 3777–3781.

48. Jia, S., Chen, Z., Zhang, N., Tan, Y., Liu, Y., Deng, J., and Yan, H. (2018). Organocatalytic enantioselective construction of axially chiral sulfone-containing styrenes. J. Am. Chem. Soc. *140*, 7056–7060.

49. Zheng, S.C., Wang, Q., and Zhu, J. (2019). Catalytic atropenantioselective heteroannulation between isocyanoacetates and alkynyl ketones: synthesis of enantioenriched axially chiral 3-arylpyrroles. Angew. Chem. Int. Ed. *58*, 1494–1498.

50. He, Y.P., Wu, H., Wang, Q., and Zhu, J. (2020). Palladium-catalyzed enantioselective Cacchi reaction: asymmetric synthesis of axially chiral 2,3-disubstituted indoles. Angew. Chem. Int. Ed. *59*, 2105–2109.

51. Luo, J., Zhang, T., Wang, L., Liao, G., Yao, Q.J., Wu, Y.J., Zhan, B.B., Lan, Y., Lin, X.F., and Shi, B.F. (2019). Enantioselective synthesis of biaryl atropisomers by Pd-catalyzed C–H olefination using chiral spiro phosphoric acid ligands. Angew. Chem. Int. Ed. *58*, 6708–6712.

52. Liao, G., Chen, H.M., Xia, Y.N., Li, B., Yao, Q.J., and Shi, B.F. (2019). Synthesis of chiral aldehyde catalysts by Pd-catalyzed atroposelective C–H naphthylation. Angew. Chem. Int. Ed. *58*, 11464–11468.

53. Jiang, F., Chen, K.W., Wu, P., Zhang, Y.C., Jiao, Y., and Shi, F. (2019). A strategy for synthesizing axially chiral naphthyl-indoles: catalytic asymmetric addition reactions of racemic substrates. Angew. Chem. Int. Ed. *58*, 15104–15110.

54. Deng, R., Xi, J., Li, Q., and Gu, Z. (2019). Enantioselective carbon-carbon bond cleavage for biaryl atropisomers synthesis. Chem *5*, 1834–1846.

55. Shen, D., Xu, Y., and Shi, S.L. (2019). A bulky chiral N-heterocyclic carbene palladium catalyst enables highly enantioselective Suzuki-Miyaura cross-coupling reactions for the synthesis of biaryl atropisomers. J. Am. Chem. Soc. *141*, 14938–14945.

56. Witzig, R.M., Fäseke, V.C., Häussinger, D., and Sparr, C. (2019). Atroposelective synthesis of tetra-ortho-substituted biaryls by catalyst-controlled non-canonical polyketide cyclizations. Nat. Catal. *2*, 925–930.

57. Wang, Y.-B., Yu, P., Zhou, Z.P., Zhang, J., Wang, J., Luo, S.H., Gu, Q.S., Houk, K.N., and Tan, B. (2019). Rational design, enantioselective synthesis and catalytic applications of axially chiral EBINOLs. Nat. Catal. *2*, 504–513.

58. Kočovský, P., Vyskočil, S., and Smrčina, M. (2003). Non-symmetrically substituted 1,1′-binaphthyls in enantioselective catalysis. Chem. Rev. *103*, 3213–3246.

59. Ding, K., Li, X., Ji, B., Guo, H., and Kitamura, M. (2005). Ten years of research on NOBIN chemistry. Curr. Org. Syn. *2*, 499–545.

60. Qi, L.-W., Li, S., Xiang, S.H., Wang, J., and Tan, B. (2019). Asymmetric construction of atropisomeric biaryls via a redox neutral cross-coupling strategy. Nat. Catal. *2*, 314–323.

61. Smrčina, M., Vyskocil, S., Maca, B., Polasek, M., Claxton, T.A., Abbott, A.P., and Kocovsky, P. (1994). Selective cross-coupling of 2-naphthol and 2-naphthylamine derivatives. A facile synthesis of 2,2′,3-trisubstituted and 2,2′,3,3′-tetrasubstituted 1,1′-binaphthyls. J. Org. Chem. *59*, 2156–2163.

62. Zheng, Z., Cao, Y., Chong, Q., Han, Z., Ding, J., Luo, C., Wang, Z., Zhu, D., Zhou, Q.L., and Ding, K. (2018). Chiral cyclohexyl-fused spirobiindanes: practical synthesis, ligand development, and asymmetric catalysis. J. Am. Chem. Soc. *140*, 10374–10381.